Network Simulation of Passive Optical Broadcast-and-Select Network for Avionics Applications

Qi Li[1,2], Robert Hendry[2], Johnnie Chan[2], Keren Bergman[2], Madeleine Glick[3], Raj Dutt[1,3]

1: PhotonIC Corporation, 5800 Uplander Way, Culver City, CA 90230, USA

2: Department of Electrical Engineering, Columbia University, 500 W. 120th Street, New York, NY 10027, USA

3: APIC Corporation, 5800 Uplander Way, Culver City, CA 90230, USA

ql2163@columbia.edu

Abstract: *A passive optical broadcast-and-select network is explored to meet stringent bandwidth, power, and latency demands of avionics applications. Models were constructed in the PhoenixSim simulation platform. The optical network is compared with an electrical network and significant improvements in network performance, power, and latency are shown.*

Keywords: Optical interconnect; Avionics; Network architecture; System simulation.

Introduction

High performance avionics systems are increasingly using multiprocessors for data processing, which require high bandwidth communication links between the compute nodes and the external sensors [1]. With the high bandwidth requirement of data processing applications and the low latency requirement of control signals, fiber optics interconnection networks present a potentially attractive platform. Interconnects based on fiber optics have advantages such as high bandwidth, low latency, EMI immunity and low weight, which have been proven in the telecommunication industry. Different from the telecommunication industry, avionics systems have additional requirements pertaining to reliability, power consumption, package size, and tolerance to extreme environments of temperature variation and vibration.

Photonic system modeling and simulation tools are important for exploring the design space, optimizing device parameters, and reducing the cost and time of development, in a similar fashion to electrical computer-aided design (CAD) tools. Using these tools, the key advantages of inserting optical interconnects in realistic systems can be evaluated for various applications.

The optical wavelength-division multiplexing (WDM) network that is studied in this paper has a passive broadcast-and-select network architecture with 32 compute nodes. Each compute node has one transmitter unit, an arrayed waveguide grating (AWG), and 32 photodetectors. The compute nodes are connected by a passive star coupler, which will broadcast any message that is received to all output fiber ports. This passive broadcast-and-select network architecture has advantages that include data rate and modulation format transparency, high reliability, and ease of maintenance. For an avionics system which may need to communicate with different external sensors with disparate protocols, the format transparency presents an especially attractive solution. The simple and completely passive star coupler also presents a robust solution with high reliability. In addition, the data rate transparency of this passive network architecture leaves room for future expansion and upgrade.

Network Simulations in PhoenixSim

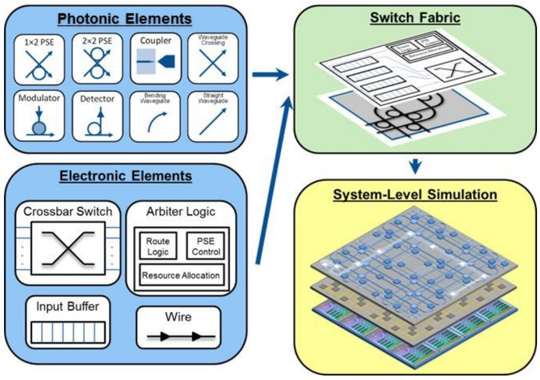

Figure 1. PhoenixSim Simulation Hierarchy

PhoenixSim (Fig.1) is a software tool that enables design space exploration of photonic interconnection networks through low-level, event-driven simulations. PhoenixSim includes a library of electronic and silicon photonic device models which can compose network-on-chips (NoCs), and chip-to-chip interconnect networks. The primary purpose of PhoenixSim is to reveal the effects of integrating silicon photonic devices into interconnection networks. Recent work has focused on using PhoenixSim to show the benefits and tradeoffs of optically-enhanced network architectures [2, 3].

PhoenixSim models photonic devices using a relatively high level of abstraction by establishing device parameters that are essential for the system level understanding of a photonic interconnection network. The silicon photonic device models include microring modulator, microring switch, and Ge photodetector [4, 5], which has been proposed to be used in applications including NoCs [6], optical network unit (ONU) [7], as well as large scale computing systems [8]. Device characteristics such as insertion loss and propagation latency are abstracted to describe the photonic devices, which can be determined experimentally or by projection.

Electrical System Model

In order to quantify the performance improvements gained with a silicon photonic network, we simulate a baseline network for comparison which represents the current electrically switched network in avionics systems.

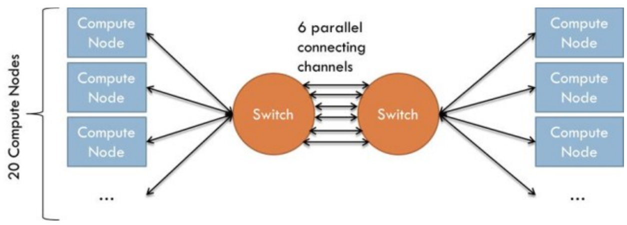

Figure 2. Layout of Electrical Baseline Simulation Model

The baseline model (Fig.2) consists of 40 processing nodes interconnected by two 26-radix switches, as shown in the illustration above. Each channel is a 2-Gb/s fiber optic transceiver. The switches use simple algorithmic routing, input and output buffering, and virtual channels. The sizes of the buffers and number of virtual channels, however, are not fixed; these parameters are included in the design space. In our preliminary results, each buffer has a size of 255 flits, with 64-bit flits, and virtual channels are not used (i.e. there is one "virtual" channel). The processors and network interfaces are able to handle application traffic at 2.5 GHz, while the network clocks operate at 2 GHz. This switch model is preliminary, and does not yet include all of the characteristics of a commercial switch (e.g. memory access latencies within the switch board). It is currently being refined for more precise simulations.

The ideal network bandwidth for this system with uniformly distributed random traffic can be calculated:

$$\frac{40 \text{ links } \times 2 \text{ Gb/s/link}}{2} + 12 \text{ links } \times 2 \text{ Gb/s/link} = 64 \text{ Gb/s}$$

This calculation consists of the sum of two terms to produce the resulting 64 Gb/s. The left term states that half of the traffic in the network will be communicated to processors that can communicate on a common switch (single hop), and while the right term describes the other half of the traffic that must traverse the intermediate links (two hops). The intermediate links act as a bottleneck for the traffic since it provides less bandwidth than what is offered by the nodes.

Optical Network Model

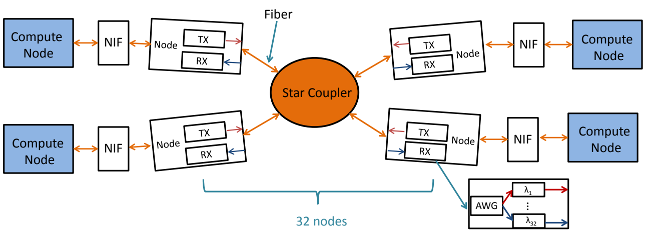

Figure 3. Optical Network Architecture in PhoenixSim

Each node in the optical network (Fig. 3) has a tunable transmitter emitting at a fixed wavelength and 32 photodetectors. The use of a tunable transmitter enables each TxRx node to have identical hardware. The output of all the transmitters is combined in a passive star coupler and distributed to all the receivers. The Network Interface (NIF) module implements the communication protocols between the processor models and the network. The NIF translates the compute node communication events into network messages and processes incoming messages it receives from network by passing the encapsulated data to the compute node. Since our network is a broadcast-and-select network architecture, each node is capable of receiving messages that are not intended for it. The NIF is responsible for checking the destination address of each message it receives and discarding those that do not have the correct address.

We assume an input laser power of 10 dBm and transmitter insertion loss of 7 dB, for a chip output optical power of 3 dBm. The transmitter unit has a data rate of 10-Gb/s. The multichannel receiver [9] in each node has a single fiber input containing up to 32 WDM signals, an AWG for demultiplexing the 32 signals to separate waveguide channels, and corresponding 32 photodetectors. The additional optical-to-electronic and electronic-to-optical conversion latency, on the order of a few nanoseconds [10], is negligible compared with the fiber delay.

The star coupler broadcasts the optical signal from each input fiber to each of the 32 output fibers. Since the optical signals occupy different wavelengths, they can be broadcasted to the same output without collision. The insertion loss for the 32 output split of any input signal is set to be 15 dB as in a similar study [11]. The latency of the star coupler is only the propagation latency of light through it, making it negligible compared with the fiber propagation latency.

Fiber channels connect each node to the central passive star coupler. We simulate 30-meter fiber length, a long fiber length for this avionics application to study the worst case latency. Fiber propagation loss for light in single-mode fiber is 0.2 dB/km, so the propagation loss is only 0.006 dB per fiber. Assuming the propagation speed of light in the fiber is 2×108 m/s, fiber latency is 5 ns/m.

Network Performance Comparison

Simulation results of average message latency and network throughput for both networks under varying traffic loads and different message sizes are plotted in Fig. 5 for comparison. The plot uses random traffic pattern with a simulation time of 0.1 ms, where each node randomly selects a destination node (uniformly), and messages arrive as a Poisson process. Random traffic is considered as a fair approximation of command-and-control type of traffic in typical avionics applications. The electrical network throughput saturates before the ideal bandwidth because of buffer contention in the electrical switch. The optical network, however, is able to closely approach the ideal network bandwidth. The optical network is also able to achieve lower latency due to higher data rate and the absence of active switching. At low traffic load, the average message latency closely reflects the physical layer latency of the network, which is primarily composed of transmission latency and propagation latency. When offered throughput approaches the network bandwidth, the increase of average message latency reflects the additional processing and queuing latency in the simulated NIF module.

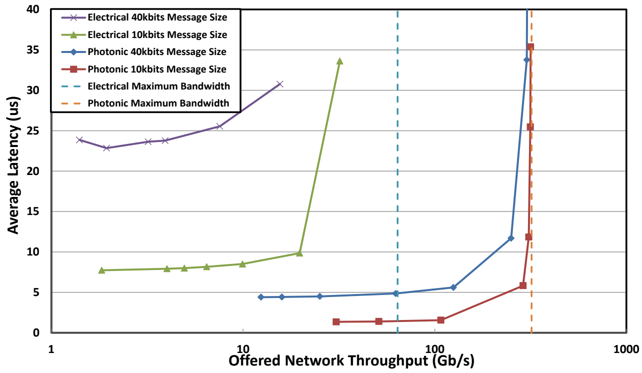

Figure 4. Latency vs. Throughput Comparison

Table 1. Optical network is compared with two different scenarios: all 32 photodetectors powered on (I), and only one photodetector on (II). (References are to typical devices)

		Electrical	Optical (I)		Optical (II)	
Component power (W)		VCSEL	With heating	Athermal	With heating	Athermal
Electrical switch		100[12]				
VCSEL transceiver @2Gb/s		0.5[13]				
HIP TX @10Gb/s			10[14]	10	10	10
HIP RX@10 Gb/s	AWG thermal stabilization		5[15]	0[16]	5	0
	ASIC (per TIA)		0.1	0.1	0.1	0.1
Total power		246	582.4	422.4	483.2	323.2
Ideal bandwidth (Gb/s)		46	320	320	320	320
pJ/bit		5347	1820	1320	1510	1010

Power Comparison

The power consumption of the electrical baseline network is compared with the optical passive star network with component power listed in Table. 1. The electrical baseline network uses VCSEL transceivers [13] and multimode fiber to connect compute nodes and the electrical switch [12]. We consider 10W power consumption for transmitter which includes redundant laser modules [14]. The optical passive star network is compared using different technologies for temperature stabilization of the AWG: a receiver with heating elements [15], and an athermal AWG [16]. Since in practice the communicating patterns of compute nodes can be known in advance, the photodetectors do not have to be powered on all the time. Here two scenarios in which all the photodetectors are always on and only one photodetector of each compute node is on are considered, representing the upper and lower bound of power consumption. The optical network has better energy efficiency in terms of pJ/bit, and this advantage is projected to be larger with future receiver technologies.

Conclusion

We model and study the electrical switched and optical passive networks for avionics applications using PhoenixSim. These networks are based on off-the-shelf and near-term devices. The network performance and power comparison results show that the optical passive network outperforms the baseline electrical network in terms of throughput, power, and latency.

References

1. Habiby, S.F.; Hackert, M.J.; , "Ronia results: WDM-based optical networks in aircraft applications," *Avionics, Fiber-Optics and Photonics Technology Conference, 2008 IEEE* , vol., no., pp.71-72, Sept. 30 2008-Oct. 2 2008.
2. J. Chan, G. Hendry, K. Bergman, L. P. Carloni, "Physical-Layer Modeling and System-Level Design of Chip-Scale Photonic Interconnection Networks," *IEEE Transactions on Computer-Aided Design of Integrated Circuits and Systems,* 30 (10) 1507-1520 (Oct 2011).
3. G. Hendry, E. Robinson, V. Gleyzer, J. Chan, L. P. Carloni, N. Bliss, K. Bergman, "Time-division-multiplexed arbitration in silicon nanophotonic networks-on-chip for high-performance chip multiprocessors ," *Journal of Parallel and Distributed Computing*, 71 (5) 641-650 (May 2011).
4. Li, Qi, et al. "Experimental characterization of the optical-power upper bound in a silicon microring modulator." *Optical Interconnects Conference*, 2012 IEEE.
5. Xu, Lin, et al. "40-Gb/s DPSK data transmission through a Silicon microring switch." *Photonics Technology Letters, IEEE*, 24.6 (2012): 473-475.
6. Xie, Yiyuan, et al. "Crosstalk noise and bit error rate analysis for optical network-on-chip." *Design Automation Conference (DAC), 2010 47th ACM/IEEE.* IEEE, 2010.
7. Xu, Lin, et al. "Colorless Optical Network Unit Based on Silicon Photonic Components for WDM PON." *Photonics Technology Letters, IEEE,* 24.16 (2012): 1372-1374.
8. Zhang, Wenjia, et al. "Broadband Silicon Photonic Packet-Switching Node for Large-Scale Computing Systems." *Photonics Technology Letters, IEEE,* 24.8 (2012): 688-690.
9. Y. Kuo, M. Kwakernaak, X. Sun, J. Pescatore, M. Gilmer, J. Oakley, Z. Ji, and A. Nikolov, "Integrated Multi-Wavelength Silicon Germanium High Speed Receivers," *IPRSN*, 2010.
10. Nishimura, S.; Inoue, H.; Hanatani, S.; Matsuoka, H.; Yokota, T.; , "Optical interconnections for the massively parallel computer," *Photonics Technology Letters, IEEE* , vol.9, no.7, pp.1029-1031, July 1997.
11. Whaley, Gregory J.; Karnopp, Roger J., "Air Force highly integrated photonics program: development and demonstration of an optically transparent fiber optic network for avionics applications", *Proc. SPIE 7700, Enabling Photonics Technologies for Defense,*

Security, and Aerospace Applications VI, 77000A (April 16, 2010);.

12. Cisco MDS 9134 Multilayer Fabric Switch. http://www.cisco.com/en/US/prod/collateral/ps4159/ps6409/ps4358/product_data_sheet0900aecd80692efd.pdf
13. JDSU RoHS-compliant SFP transceiver. http://www.jdsu.com/ProductLiterature/plrxpl-vi-s24-22-ds-oc-ae.pdf
14. JDSU Integrable Tunable Laser Assemblies. http://www.jdsu.com/ProductLiterature/5205t-5206t-itla-ds-cms-ae.pdf
15. Toyoda, S.; Kaneko, A.; Ooba, N.; Yamada, H.; Kurihara, T.; Okamoto, K.; Imamura, S.; , "Polarization-independent low-crosstalk polymeric AWG-based tunable filter operating around 1.55 µm," *Photonics Technology Letters, IEEE ,* vol.11, no.9, pp.1141-1143, Sept. 1999
16. NeoPhotonics Athermal Wideband AWG MUX/DEMUX. http://www.neophotonics.com/_upload/pro/2010-09-19/c46d7858-07df-4359-8110-d0980f881f32.pdf.